World Academy of Science, Engineering and Technology
International Journal of Physical and Mathematical Sciences
Vol:16, No:11, 2022

Finite Element Approximation of the Heat Equation under Axisymmetry Assumption

Raphael Zanella

Abstract—This works deals with the finite element approximation of axisymmetric problems. The weak formulation of the heat equation under axisymmetry assumption is established for continuous finite elements. The weak formulation is implemented in a C++ solver with implicit time marching. The code is verified by space and time convergence tests using a manufactured solution. An example problem is solved with an axisymmetric formulation and with a 3D formulation. Both formulations lead to the same result but the code based on the axisymmetric formulation is mush faster due to the lower number of degrees of freedom. This confirms the correctness of our approach and the interest of using an axisymmetric formulation when it is possible.

Keywords—Axisymmetric problem, continuous finite elements, heat equation, weak formulation.

I. Introduction

WHEN the geometry of the system, the source terms and the initial/boundary conditions are roughly symmetric with respect to a certain axis, it may be interesting to treat the problem as axisymmetric due to the substantial cut in the computational cost that results. This configuration may arise in applications such as moisture and heat transfer in a reactor vessel [1], induction heating [2] or cylindrical bodies at high temperature in machine parts [3]. It is nevertheless not trivial to derive the weak formulation that needs to be solved when this choice is made. The problem is still 3D but the solution depends on the two cylindrical coordinates (r, z) only. Following the arguments used in the work [4] on the compressible Euler equations, we establish the axisymmetric weak formulation for the heat equation. We then present an illustrative numerical result which shows the computational efficiency of an axisymmetric formulation with respect to a (full) 3D formulation.

We consider homogeneous Dirichlet boundary conditions. Denoting by Ω the axisymmetric computational domain, by $\partial\Omega$ its boundary (the boundary of a domain is always indicated by the symbol ∂ in the article) and by $T > 0$ the time limit, the problem is expressed

$$\begin{cases} \partial_t u - \nabla\cdot(\kappa\nabla u) = f & \text{in } \Omega \times [0,T], \\ u = 0 & \text{on } \partial\Omega \times [0,T], \\ u_{|t=0} = u_0 & \text{in } \Omega, \end{cases} \tag{1}$$

where u is the unknown solution field, κ is the diffusivity parameter, f is an axisymmetric source term and u_0 is an axisymmetric initial condition.

R. Zanella is with the Oden Institute for Computational Engineering and Sciences, University of Texas, Austin, TX 78712 USA (e-mail: zanella@oden.utexas.edu).

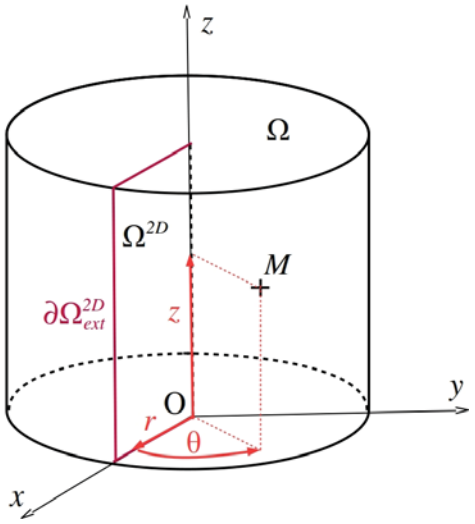

Fig. 1 Example of cylindrical domain of computation Ω and the associated meridian section Ω^{2D}. A point $M \in \Omega$ is located by its cylindrical coordinates (r, θ, z), with $(r, z) \in \Omega^{2D}$ and $\theta \in [0, 2\pi)$

II. Axisymmetric Weak Formulation

We assume that we look for an axisymmetric solution. One needs to define an appropriate function space of approximation. We use the cylindrical coordinates (r, θ, z). Let us note Ω^{2D} the half-meridian section, say at $\theta = 0$, of Ω. We denote by $\partial\Omega^{2D}_{ext} = \partial\Omega^{2D} \cap \partial\Omega$ the exterior boundary of Ω^{2D}. An illustration is presented in Fig. 1. We denote by $\mathcal{T}_h$ a mesh of Ω^{2D} with characteristic mesh size h. A cell of $\mathcal{T}_h$ is denoted by K. In order to build the approximation space, we define the space

$$V_h^{2D} = \left\{ v_h \in \mathcal{C}^0\left(\overline{\Omega^{2D}}; \mathbb{R}\right) ;\, v_{h|_K} \in \mathbb{P}_p,\, \forall K \in \mathcal{T}_h, \right. \\ \left. \text{and } v_h = 0 \text{ on } \partial\Omega^{2D}_{ext} \right\}, \tag{2}$$

where $p \in \mathbb{N}^*$ is the order of the polynomial approximation. The approximation space is

$$V_h = \left\{ v_h \in \mathcal{C}^0\left(\overline{\Omega}; \mathbb{R}\right) ;\, \exists v_h^{2D} \in V_h^{2D}; \right. \\ \left. v_h(r,\theta,z) = v_h^{2D}(r,z),\, \forall (r,\theta,z) \right\}. \tag{3}$$

The functions of V_h are axisymmetric by definition. One can verify that they also satisfy $v_{h|\partial\Omega} = 0$.

The approximate weak formulation is obtained by multiplying the first line of (1) by a test function and by then integrating over Ω. The divergence theorem and the fact the test functions cancel on $\partial\Omega$ allow to re-write the diffusive

term. We can finally express the weak formulation as: find $u_h \in \mathcal{C}^1([0,T];V_h)$ such that

$$\begin{cases} \int_\Omega \frac{du_h}{dt}(t)v_h dV + \int_\Omega \kappa \nabla u_h(t)\cdot\nabla v_h dV = \int_\Omega f(t)v_h dV, \\ \qquad \forall t\in[0,T],\ \forall v_h \in V_h, \\ u_h(0) = u_{0h}, \end{cases} \tag{4}$$

where $u_{0h} \in V_h$ is an approximation of u_0. Note that we have not used the axisymmetry assumption yet.

Let g be a function defined in Ω. Because Ω is axistmmetric, we can express the integral over Ω as the integral over Ω^{2D} of the integral over the azimuthal direction (i.e. over a ring of coordinates $(r,z)\in\Omega^{2D}$):

$$\int_\Omega g dV = \int_{\Omega^{2D}} \left(\int_{\theta=0}^{2\pi} g r d\theta \right) dS. \tag{5}$$

The elementary volume is $dV = r dr d\theta dz$ and the elementary surface is $dS = dr dz$. Let us assume that g is axisymmetric. We have then

$$\int_{\theta=0}^{2\pi} g(r,\theta,z) r d\theta = 2\pi g^{2D}(r,z) r,\ \forall (r,z)\in\Omega^{2D}, \tag{6}$$

where $g^{2D} \equiv g_{|\Omega^{2D}}$. By combining (5) and (6), we can write

$$\int_\Omega g dV = 2\pi \int_{\Omega^{2D}} g^{2D} r dS. \tag{7}$$

This formula will allow us to simplify the weak formulation (4).

The trial function, the test functions and the source term are axisymmetric so we can apply (7) to every term of the first line of (4). Note that, in particular due to axisymmetry,

$$\begin{aligned} \nabla u_h \cdot \nabla v_h = \partial_r u_h \partial_r v_h + \partial_z u_h \partial_z v_h = \\ \partial_r u_h^{2D} \partial_r v_h^{2D} + \partial_z u_h^{2D} \partial_z v_h^{2D} = \nabla u_h^{2D} \cdot \nabla v_h^{2D}, \end{aligned} \tag{8}$$

where u_h^{2D} and v_h^{2D} are the functions defined in Ω^{2D} associated to u_h and v_h according to definition (3). Looking for $u_h \in V_h$ is equivalent to looking for the associated $u_h \in V_h^{2D}$. Testing by every $v_h \in V_h$ is equivalent to testing by the 3D-extension of every $v_h^{2D} \in V_h^{2D}$. Considering all of this, we can equivalently express (4) as: find $u_h^{2D} \in \mathcal{C}^1([0,T];V_h^{2D})$ such that

$$\begin{cases} \int_{\Omega^{2D}} \frac{du_h^{2D}}{dt}(t) v_h^{2D} r dS + \int_{\Omega^{2D}} \kappa \nabla u_h^{2D}(t)\cdot\nabla v_h^{2D} r dS = \\ \qquad \int_{\Omega^{2D}} f^{2D}(t) v_h^{2D} r dS,\ \forall t\in[0,T],\ \forall v_h^{2D} \in V_h^{2D}, \\ u_h^{2D}(0) = u_{0h}^{2D}, \end{cases} \tag{9}$$

where $f^{2D} \equiv f_{|\Omega^{2D}}$ and $u_{0h}^{2D} \in V_h^{2D}$ is an approximation of $u_{0|\Omega^{2D}}$. The weak formulation (9), referred as axisymmetric weak formulation in this article, is similar to that of a 2D heat equation with homogeneous Dirichlet boundary conditions except for the r factor in every term and the fact that the trial and test functions are not necessarily zero at the axis, i.e. the fact that only the exterior boundary of Ω^{2D} is a Dirichlet boundary.

III. Matrix Form of the Weak Formulation

Let $\{\varphi_i\}_{i\in[|1,n_{dof}|]}$ be a basis for V_h^{2D}, with $n_{dof} \in \mathbb{N}^*$ the number of degrees of freedom. We denote by $U \in \mathcal{C}^1([0,T];\mathbb{R}^{n_{dof}})$ the vector function containing the degrees of freedom of u_h^{2D}:

$$u_h^{2D}(t) = \sum_{j=1}^{n_{dof}} U_j(t)\varphi_j,\ \forall t\in[0,T]. \tag{10}$$

We denote by $U^0 \in \mathbb{R}^{n_{dof}}$ the vector containing the degrees of freedom of u_{0h}^{2D}.

The weak formulation (9) is equivalent to the system of ODEs: find $U \in \mathcal{C}^1([0,T];\mathbb{R}^{n_{dof}})$ such that

$$\begin{cases} M\frac{dU}{dt}(t) + KU(t) = F(t),\ \forall t\in[0,T], \\ U(0) = U^0, \end{cases} \tag{11}$$

where $M \in \mathbb{R}^{n_{dof}\times n_{dof}}$ is the mass matrix defined by

$$M_{ij} = \int_{\Omega^{2D}} \varphi_j \varphi_i r dS,\ \forall (i,j)\in[|1,n_{dof}|]^2, \tag{12}$$

$K \in \mathbb{R}^{n_{dof}\times n_{dof}}$ is the stiffness matrix defined by

$$K_{ij} = \int_{\Omega^{2D}} \kappa \nabla\varphi_j \cdot \nabla\varphi_i r dS,\ \forall (i,j)\in[|1,n_{dof}|]^2, \tag{13}$$

and $F \in \mathcal{F}([0,T];\mathbb{R}^{n_{dof}})$ is the vector source term defined by

$$F_i(t) = \int_{\Omega^{2D}} f^{2D}(t)\varphi_i r dS,\ \forall i\in[|1,n_{dof}|],\ \forall t\in[0,T]. \tag{14}$$

Note the presence of the r factor in all of the coefficients and the fact that all the φ_i are not zero at the axis.

IV. Time Discretization

The time approximation of (11) is constructed by using an implicit Euler scheme. Let $N \in \mathbb{N}_*$. We denote by $\Delta t = T/n$ the time step and we note $t_n = n\Delta t$, $\forall n \in [|0,N|]$. We denote by u_h^n and U^n an approximation of $u_h(t_n)$ and $U(t_n)$, respectively. We note

$$u_{\Delta t} = (u_{|t=t_n})_{n\in[|0,N|]},\ u_{h\Delta t} = (u_h^n)_{n\in[|0,N|]}. \tag{15}$$

After initializing U^0, the algorithm consists in solving for every $n \geq 0$:

$$\begin{cases} k^{n+1} = A^{-1}(-KU^n + F(t_{n+1})), \\ U^{n+1} = U^n + k^{n+1}\Delta t, \end{cases} \tag{16}$$

where k^{n+1} is an approximation of $\frac{dU}{dt}(t_{n+1})$ and

$$A = M + \Delta t K. \tag{17}$$

The algorithm is implemented in a C++ code based on the MFEM library for finite elements [5].

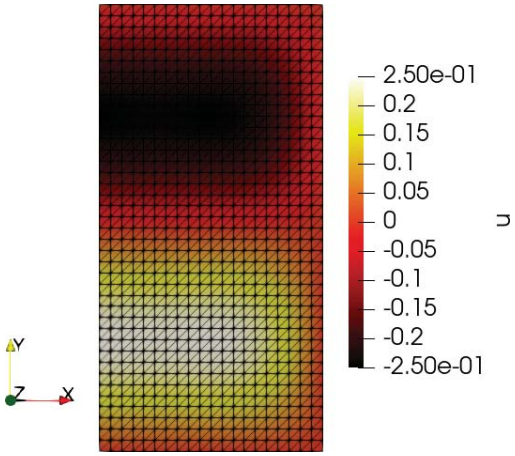

Fig. 2 Manufactured solution field in Ω^{2D} at $t = 1$. The symmetry axis is the left vertical border (r axis = X axis, z axis = Y axis). Parameters: $\kappa = 2$, $h = 0.025$, $\Delta t = 10^{-4}$

V. Verification on a Manufactured Solution

Before solving an actual problem, we verify that the space and time approximations are correctly implemented by performing a convergence test on a manufactured solution. We consider the cylindrical domain

$$\Omega = \{(r, \theta, z) \in \mathbb{R}^3;\ 0 \leq r < 0.5,\ 0 \leq \theta < 2\pi,\ 0 < z < 1\} \tag{18}$$

and the manufactured solution

$$u(r, \theta, z, t) = (r^2(\sin(2\pi r) - 1) + 0.25)\sin(2\pi z)\cos(2\pi t). \tag{19}$$

An illustration of the solution is presented in Fig. 2. f and u_0 are set so that u defined in (19) is solution of (1):

$$f = \partial_t u - \nabla\cdot(\kappa\nabla u) \tag{20}$$

and

$$u_0(r, \theta, z) = (r^2(\sin(2\pi r) - 1) + 0.25)\sin(2\pi z). \tag{21}$$

The convergence test is performed on the norm

$$\|u_{\Delta t} - u_{h\Delta t}\|_{l^\infty} = \max_{0 \leq n \leq N} \|u_{|t=t_n} - u_h^n\|_{L^2(\Omega)}. \tag{22}$$

The L^2-norm is computed over Ω but computing it over Ω^{2D} does not change the conclusion of the convergence test. The mesh is triangular. The order of the polynomial approximation is $p = 1$.

We first study the evolution of the error with the mesh size. We use a rather strong diffusivity to weaken the importance of the time derivative term and we fix the time step to a very small value. The time step error is then neglectable compared to the mesh size error. The results are presented in Tab. I. The computed order of convergence (COC) converges toward $k + 1 = 2$, which is consistent with the theory. See Theorem 6.29 in [6, p. 296].

We then study the evolution of the error with the time step. We use a rather weak diffusivity to strengthen the importance of the time derivative term and we fix the mesh size to a very small value. The mesh size error is then neglectable compared to the time step error. The results are presented in Tab. II. The COC converges toward 1, which is consistent with the theory, see the same theorem.

TABLE I
Mesh Size Convergence Test

h	$\|u_{\Delta t} - u_{h\Delta t}\|_{l^\infty}$	COC
0.1	0.012280034	-
0.05	0.0032256946	1.929
0.025	0.00081782067	1.98
0.0125	0.00020608841	1.989

Diffusivity $\kappa = 2$. Fixed small time step $\Delta t = 10^{-4}$. Time limit $T = 1$

TABLE II
Time Step Convergence Test

Δt	$\|u_{\Delta t} - u_{h\Delta t}\|_{l^\infty}$	COC
0.1	0.023979616	-
0.05	0.012747723	0.912
0.025	0.0066965764	0.929
0.0125	0.0034543529	0.955

Diffusivity $\kappa = 0.1$. Fixed small mesh size $h = 0.0125$. Time limit $T = 1$

VI. Comparison of the Axisymmetric Formulation with a 3D Formulation

The goal of this section is to compare the solution given by the code based on the axisymmetric weak formulation and that given by a code based on a 3D weak formulation, i.e. a weak formulation of problem (1) with trial/test functions defined in Ω and not necessary axisymmetric (but still piecewise polynomial and of the same order as for the axisymmetric weak formulation), and to compare the execution times.

A. Problem setup

We use the same domain Ω defined in (18). We define

$$\Omega_s = \{(r, \theta, z) \in \mathbb{R}^3;\ 0 \leq r < 0.35,\ 0 \leq \theta < 2\pi,\ 0.15 < z < 0.85\}, \tag{23}$$

a subdomain of Ω, and set the source term as

$$f(r, \theta, z, t) = \begin{cases} 1 & \text{in } \Omega_s \times [0, T], \\ 0 & \text{in } \Omega \setminus \Omega_s \times [0, T]. \end{cases} \tag{24}$$

The initial condition is

$$u_0(r, \theta, z) = 0 \text{ in } \Omega. \tag{25}$$

The physical problem corresponding to this setup is that of a cylindrical piece of material, initially at an uniform temperature, in which a constant heat source (generated by an electrical current for instance) is turned on at $t = 0$ while its boundaries are maintained at the initial temperature.

The axisymmetric computation is performed with a triangular mesh while the 3D computation is performed with a tetrahedral mesh, both with characteristic mesh size h. The order of the polynomial approximation is $p = 1$.

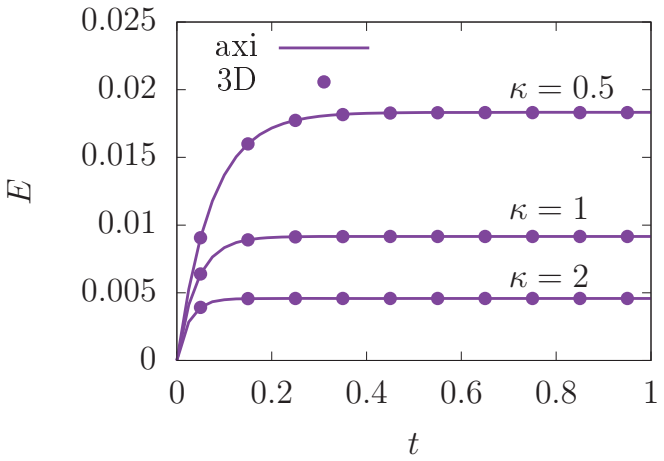

Fig. 3 Energy (see definition in (26)) as a function of time for different values of diffusivity and for axisymmetric or 3D computation

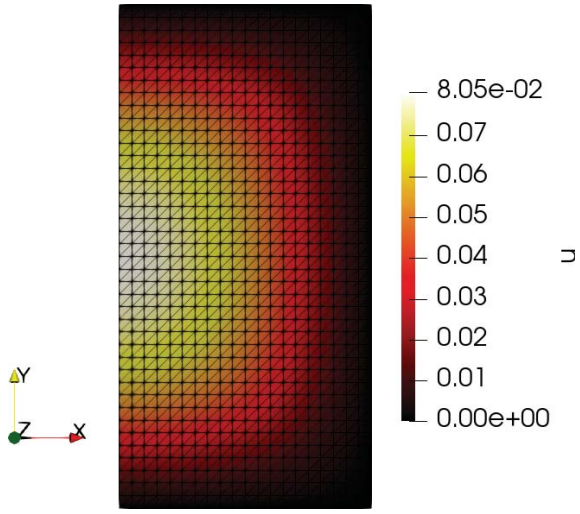

Fig. 4 Field of u in Ω^{2D} at $t = 1$ ($\kappa = 0.5$) by axisymmetric computation (r axis = X axis, z axis = Y axis)

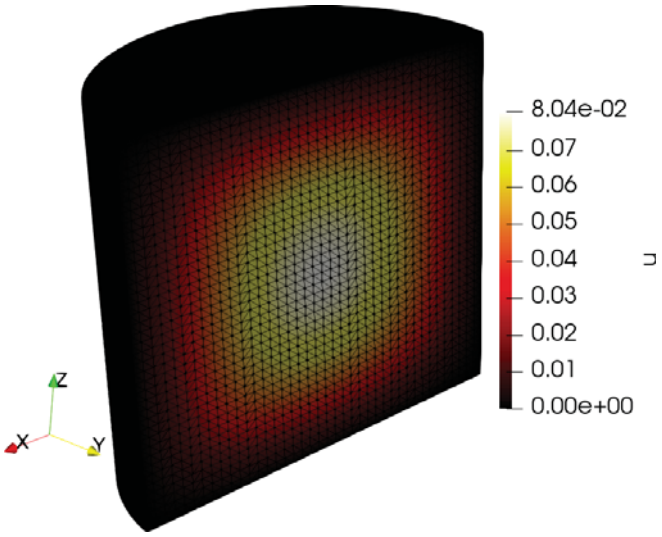

Fig. 5 Field of u in a half-section of Ω at $t = 1$ ($\kappa = 0.5$) by 3D computation

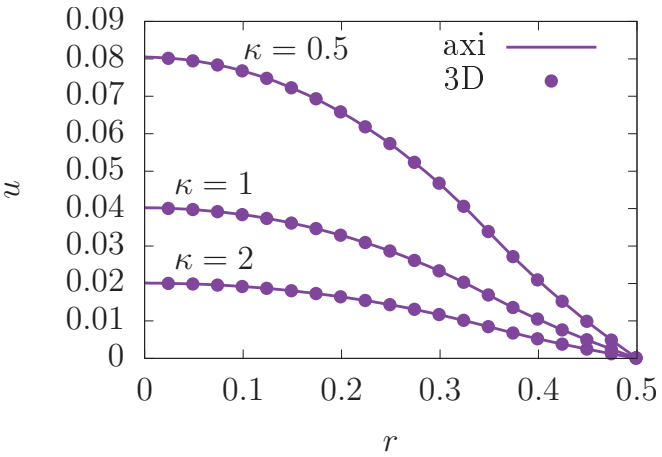

Fig. 6 Radial profile of u at $\theta = 0$, $z = 0.5$ and $t = 1$ for different values of diffusivity and for axisymmetric or 3D computation

B. Comparison of the Results

We first compare the solutions given by the axisymmetric and 3D approaches. In this subsection, we use $h = 0.025$ and $\Delta t = 0.025$. We run the computation until a steady state is reached. We know that it is the case by monitoring the energy

$$E = \int_\Omega u dV, \tag{26}$$

which then reaches a constant value, see Fig. 3. No matter the diffusivity, the axisymmetric and 3D formulations lead to a very close value of energy. The higher the diffusivity, the higher the heat transfer rate, the faster the steady regime is reached.

We compare the solutions given by the axisymmetric formulation and the 3D formulation at final time $t = 1$. The solution field is shown in Fig. 4 (axisymmetric) and Fig. 5 (3D). The fields given by both formulations are very close. The small difference, seen for the maximum value of u in the legend for instance, may be due to numerical errors. It may also be due to the fact that the tetrahedral mesh does not perfectly form a partition of Ω due to its curvature.

The profiles of the steady solution at mid-height for different diffusivities are presented in Fig. 6. These profiles confirm that the fields given by both formulations are almost identical. At steady state, the heat power that is injected is equal to the heat power that escapes the system. The higher the diffusivity, the weaker the temperature gradient needed to produce the heat flux, the lower the temperature in the central part.

C. Comparison of the Execution Times

We now compare the execution times needed by the axisymmetric and 3D codes to solve the problem (when using the same mesh size). The execution time needed by the axisymmetric code is naturally much lower than that needed by the 3D code due to the lower number of degrees of freedom involved. To illustrate this, we study the ratio of the numbers of degrees of freedom

$$R_{dof} = \frac{n_{dof} \text{ in 3D}}{n_{dof} \text{ in axi}} \tag{27}$$

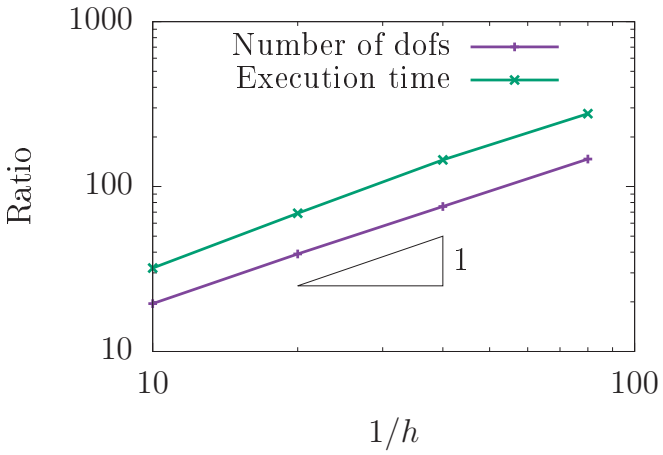

Fig. 7 Problem size and execution time ratios, between 3D and axisymmetric computations, versus inverse of the mesh size

and the ratio of the execution times, i.e. the speedup,

$$R_{time} = \frac{\text{Execution time in 3D}}{\text{Execution time in axi}} \tag{28}$$

as the mesh size varies.

We present in Fig. 7 the ratios R_{dof} and R_{time} as a function of the inverse of the mesh size. We use $\kappa = 0.5$ and $\Delta t = 0.025$. 1000 iterations are performed for every h. The computations are performed in serial to avoid any scalability effect. The execution time is the execution time of the time loop part only.

We observe that R_{dof} scales as $1/h$. This is expected because the number of degrees of freedom per dimension scales as $1/h$ and because by using an axisymmetric formulation instead of a 3D formulation one uses a mesh with a dimension of 2 instead of 3. We find that R_{time} is much larger than 1 and that it approximately scales as R_{dof}. This means that the axisymmetric approach is much faster than the 3D one and that the speedup scales as the factor of the problem size reduction, i.e. as $1/h$. This observation confirms the interest of the axisymmetric code which is computationally more efficient (and more and more efficient as h decreases).

VII. Conclusion

We have presented a methodology to derive the weak formulation of the heat equation, with homogeneous Dirichlet boundary conditions, with assumed axisymmetry. The methodology relies on the use of an approximation space of axisymmetric functions. The axisymmetry of the domain and of the trial and test functions allows to simplify the terms of the weak formulation and lead to a weak formulation similar to that of a 2D problem. The key aspects of the axisymmetric weak formulation are the r factor in every term and the treatment of the axis boundary, which is not a Dirichlet boundary. The algorithm, based on an implicit Euler time scheme, is implemented in a C++ code. A test on a manufactured solution shows the expected convergence rates in terms of mesh size and time step. The numerical example of a cylindrical solid with axisymmetric heating and initial condition illustrates the interest of the axisymmetric formulation compared to a 3D formulation. The results given by both approaches are quasi identical but the code using the axisymmetric formulation is much faster. As a matter of fact, the axisymmetric code uses a 2D mesh instead of a 3D mesh, so that the number of degrees of freedom is much lower. We find that the speedup in serial computational time when using the axisymmetric formulation scales as the inverse of the mesh size. The axisymmetric formulation would nevetheless not be able to capture a symmetry breach as the 3D formulation.

Acknowledgment

This material is based upon work supported by the Department of Energy, National Nuclear Security Administration under Award Number DE-NA0003969.

References

[1] Z. P. Bazant, J.-C. Chern and W. Thonguthai, *Finite Element Program for Moisture and Heat Transfer in Heated Concrete*, Nuclear Engineering and Design 68, pp. 61-70, 1981.
[2] C. Chaboudez, S. Clain, R. Glardon, D. Mari, J. Rappaz and M. Swierkosz, *Numerical Modeling in Induction Heating for Axisymmetric Geometries*, IEEE Transactions on Magnetics 33(1), pp. 739-745, 1997.
[3] S. V. Litvinov, L. I. Trush and A. A. Avakov, *Some Features of Temperature Field Definition in Axisymmetric Problems*, 2017 International Conference on Industrial Engineering, Applications and Manufacturing.
[4] V. A. Dobrev, T. E. Ellis, T. V. Kolev and R. N. Rieben, *High-order curvilinear finite elements for axisymmetric Lagrangian hydrodynamics*, Computers & Fluids 83, pp. 58-69, 2013.
[5] MFEM: Modular Finite Element Methods library, https://mfem.org.
[6] A. Ern and J.-L. Guermond, *Theory and Practice of Finite Elements*, 1st ed., Springer, New York, 2004.